Cluster Emission and Extremely Deformed Shapes in the N=Z Nucleus ^{44}Ti *

P. Papka, C. Beck, F. Haas, V. Rauch, M. Rousseau, P. Bednarczyk, S. Courtin, O. Dorvaux, K. Eddahbi, J. Robin, A. Sànchez i Zafra

Institut de Recherches Subatomiques, UMR7500, CNRS-IN2P3/Université Louis Pasteur, 23 rue du Loess, B.P. 28, F-67037 Strasbourg Cedex 2, France

O. Stezowski, and A. Prévost

IPN Lyon, CNRS-IN2P3/Université Lyon-1, F-69622 Villeurbanne Cedex, France

Highly excited and rapidly rotating compound nuclei (CN) produced in fusion-evaporation (FE) reactions can be well investigated by using charged particle spectroscopy. In such hot nuclei, with excitation energies as high as E^*_{CN} = 80 MeV, the spectral shapes of α particles provide information on the nuclear deformation. We report here on in-plane light charged particle (LCP) - heavy-ion (HI) coincident measurements for the ^{16}O+^{28}Si reaction. The experiment was carried out at three bombarding energies, E_{lab}(^{16}O) = 76, 96 and 112 MeV with the multidetector array ICARE at the VIVITRON Tandem facility. The Monte Carlo version of the statistical-model code CASCADE, which describes the FE process, has been used to characterize the ^{44}Ti CN. A unique set of deformability parameters reproduces well the experimental α spectra to the three bombarding energies. The discrepancies observed for the proton spectra are still to be explained.

PACS numbers: 25.70.Gh, 25.70.Jj, 25.70.Mn, 24.60.Dr

1. Introduction

The LCP spectroscopy is based upon the cumulative LCP energy spectra originating from CN decay to residual nuclei with the contribution of all the intermediate steps. The spectrum deconvolution is much simpler in the ^{44}Ti case as compared to heavier CN's, such as ^{59}Cu, ^{56}Ni or ^{67}Ga, studied in the past [1-3]. Fig. 1 displays for the ^{44}Ti CN the position of the

* Presented at the XXXVII Zakopane School of Physics, International Conference on Nuclear Physics, Trends in Nuclear Physics, Zakopane, Poland, September 3-10, 2002.

Yrast line, which defines the phase space of the light particle emission, as simulated by the statistical-model. Deformation effects lower the Yrast line and, thus, reduce the α particle energies [1,4]. It has been shown [1,2] that the transmission coefficients (T_l) can be adjusted to shift the barrier position in order to improve the agreement with the experimental data in the near-barrier region. In the high-energy part of the α spectrum, the effect of the T_l is smaller and inverted [2] compared to that of the deformability parameters (see Fig. 2). In this paper we report on the investigation of the $^{16}O+^{28}Si$ reaction which has been studied at three different bombarding energies. The results of the coincident measurements are compared to statistical-model calculations to search for deformation effects.

2. Experimental procedures and analysis

2.1. The charged particle multidetector array ICARE

The experiment was performed at the VIVITRON Tandem facility of IReS (Strasbourg) at three bombarding energies E_{lab} = 76, 96 and 112 MeV, with the multidetector array ICARE. A 200 μg/cm^2 thick natural Silicon target was used. The ΔE-E telescopes of ICARE were 40 μm thick Si(SB) detectors followed by 2 cm thick CsI(Tl) scintillators for LCP's detection. HI are detected with 4.8 cm long ionization chambers (IC) filled with 11 torr isobutane followed by a 500 μm thick Si(SB) detector. Beam intensities were kept constant to $\approx$ 5 pnA, and the vacuum was of the order of 10^{-6} torr. In addition to the standard ΔE-E discrimination, time-of-flight measurements were undertaken to discriminate LCP's stopped in the ΔE detectors allowing their energy thresholds to be lowered to $\approx$ 100 keV. Moreover the heavier particles reaching the ΔE Silicon diodes could also be eliminated from the data. The LCP telescopes were located in the Θ_{lab}=30°-130° angular range with $\Delta\Theta$=5° steps. The IC's covered angles in the forward direction from Θ_{lab}=10° to Θ_{lab}=30° with $\Delta\Theta$=5° steps. Charge discrimination could be achieved up to Z=18 for the most forward IC's. Coincident measurements using 27 LCP telescopes and 10 IC's provided a set of more than 2000 coincident E_{LCP}-E_{HI} spectra corresponding to LCP detected with their associated evaporation residues (Z=15,16,17). It is expected that such an amount of spectra is able to constrain the parameters of the statistical-model code CACARIZO described thereafter.

2.2. Brief description of the statistical-model code CACARIZO

CACARIZO, the Monte Carlo version of the statistical-model code CASCADE based on the Hauser-Feshbach formalism, describes the LCP evaporation processes [1,3,4]. To be consistent throughout the analysis, not

only the energy spectra but also the angular correlations were compared to calculations. As CACARIZO predicts spectra with statistical errors the evaluation of the final set of deformability parameters was achieved by using a standard χ^2 minimization. The main practical interest of the code is

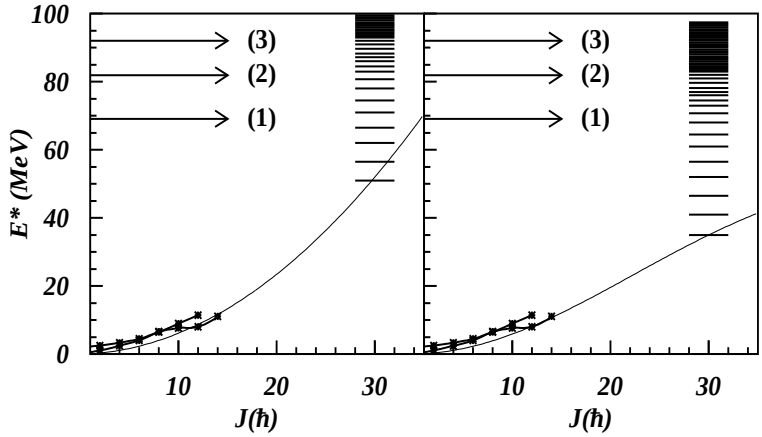

Fig. 1. Yrast line parametrizations as defined in the text (see Table 1). Excitation energies (1), (2) and (3) are the entry points in the ^{44}Ti CN for the three ^{16}O bombarding energies. The stars at low spins represent the experimental ^{44}Ti Yrast states [5].

that it offers the opportunity to calculate energy spectra in the laboratory frame, including a detailed account of experimental geometry and detector thresholds. Therefore the comparisons with data are free from a possible bias originating from the laboratory to c.m. frame transformation. Parts of the code have been extensively described elsewhere [1,3,4]. Fig. 1 shows how a more realistic Yrast line (right side) is simulated rather than the rotating liquid drop mpdel (RLDM) one [1] (left side). As a consequence the deformation in the hot rotating nuclei implies that the excitation energy, for a corresponding total angular momentum J, is lowered as compared with spherical nuclei. The Yrast parametrizations (see Eq. 1) are achieved with the two deformabity parameters δ_1 and δ_2 which fit the experimental data, their values are given in Table 1. As the level density is shifted to lower E^* the LCP emission probabilities are enhanced with a larger number of available levels. Consequently low-energy particles are more likely emitted. The other important part of the code is the T_l calculation. They are of importance in the near-barrier region where, for each light particle and at a given kinetic energy, they define the emission probability of low-energy particles to escape from the potential. Well above the barrier, the kinetic

energy is higher than the potential barrier making the T_l to be much more insensitive. The values of the critical angular momentum L_{cr} listed in Table 1 are deduced from the complete fusion cross section data [6] using the sharp cutoff model. The L-diffuseness is set equal to unity [3,4] and the level density parameter a to A/8 MeV^{-1} [7].

2.3. From effective moment of inertia to axis ratios

The Yrast line is parametrized with the deformability parameters ($\delta_{1,2}$):

$$E_J = \frac{\hbar^2}{2\mathcal{J}_{eff}} J(J+1) \qquad with \qquad \mathcal{J}_{eff} = \mathcal{J}_{sphere}(1+\delta_1^2+\delta_2^4) \quad (1)$$

where $\mathcal{J}_{eff}$ is the effective moment of inertia and $\mathcal{J}_{sphere}$ is the rigid body moment of inertia of a spherical nucleus. Assuming an ellipsoidal shape for $\mathcal{J}_{eff}$ and volume conservation, the axis ratio (Table 1), are equal to:

$$a/c = (1+\delta_1 J^2+\delta_2 J^4)^{3/2} \quad (2)$$

for an oblate shape,

$$1+(3-\gamma)x+3x^2+x^3 = 0 \;\; with \;\; x=(b/a)^2 \;\; and \;\; \gamma = 8(1+\delta_1 J^2+\delta_2 J^4)^3 \quad (3)$$

for a prolate shape. Ratios a/c and b/a are given in Table 1.

3. Discussion of the experimental results

3.1. Fitting procedures

It has been shown in several cases [2,3,4,7], that δ_1 and δ_2 may be the only parameters to be adjusted in order to describe the spectral shapes consistently. However, in some cases [1] discrepancies are still observed in the low-energy parts of the spectra where yields are systematicaly underestimated. The left side of Fig. 2 shows the need of a few MeV shift of the barrier to lower energies when the T_l are calculated with the optical model (OM). In this semi-empirical calculation, using reverse kinematics reaction data, the emitter is considered as a cold nucleus, far from excitation energies reached in CN, so that the influence of the excitation is not taken into account. The only way to solve this problem is to correct the T_l which are deformation dependent. Several authors [1,2] have shown that an increase of the OM interaction radius could be a reasonable approximation to simulate the data. For the present ^{16}O+^{28}Si reaction an increase by a factor 1.3 is sufficient. We concentrate more on the high-energy part of the spectra where the α tails are reproduced with a unique set of δ parameters almost

independently from the T_l choice. However the low-energy part of spectra has still to be better described by means of a T_l correction in the framework of excited nuclei as shown on the right side of Fig. 2. Although ^{44}Ti is fed through three different entry points the Yrast line has to be parametrized in the same way so that all of the 2000 coincident spectra are consistently compared to calculation. Moreover, In order to validate this calculation, the LCP angular distributions have also to be reproduced.

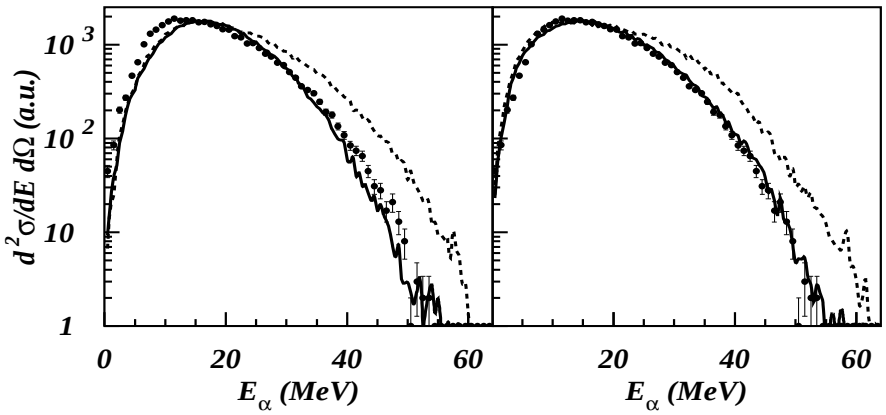

Fig. 2. Experimental (points) and calculated (lines) α spectra at E_{lab} = 96 MeV. The ER are detected at Θ_{lab}=-20°, and the α at Θ_{lab}=55°. The calculations use either the RLDM parameters (dashed) or increased deformability parameters (line) given in Table 1. The left and right sides calculated spectra use T_l from standart OM and with increased OM interaction radii, respectively, as discussed in the text.

3.2. Spectral shape of α particles

Fig. 3 illustrates how well data are reproduced for α particles with the appropriate set of parameters given in Table 1. The axis ratios are extracted from the effective moment of inertia which represents the dynamic deformation of the hot rotating nuclei populated at the critical angular momentum (Eqs. 1-3). The axis ratios reported in Table 1 indicate strong deformation effects for both oblate and prolate assumptions of the ^{44}Ti CN. Here the possible coexistence of more exotic shapes is not considered.

3.3. Spectral shapes of protons

Despite the fact that the α spectra are well reproduced, the behaviour of the proton spectra shown in Fig. 4 is far from being understood. This is to be contrasted to other experiments carried out in neighbouring systems

for which both α's and protons are simultaneously well reproduced [4,7]. However such large discrepancies have already been observed in our previ-

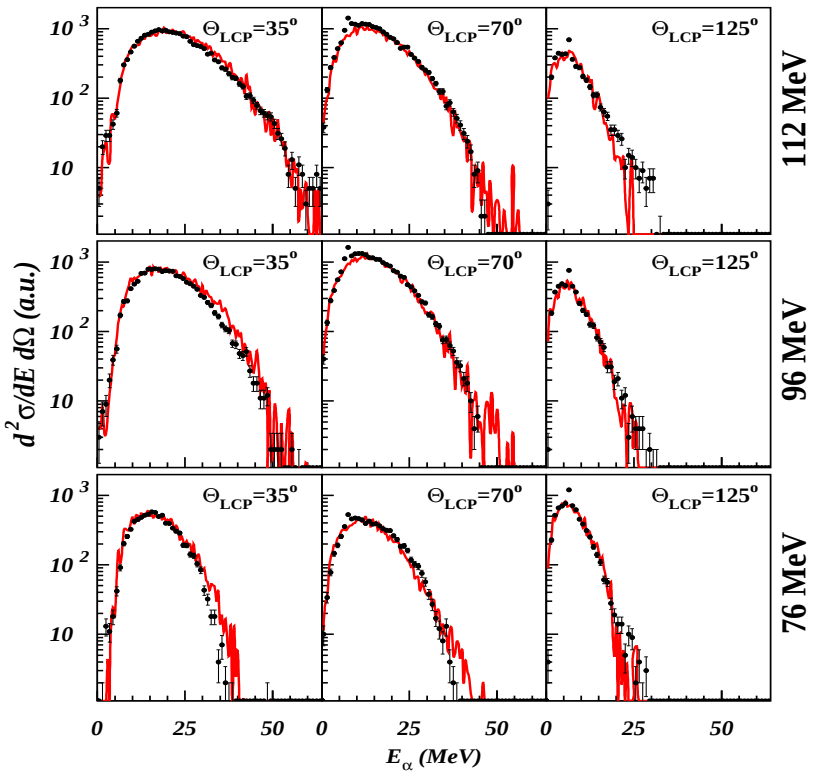

Fig. 3. Experimental (points) and calculated (solid lines) α spectra for the three ^{16}O bombarding energies. The HI's are detected at Θ_{lab}=-15° with α's being emitted in coincidence at the indicated angles. Calculations were carried out with the parameter set of Table 1.

ous investigation of the ^{28}Si+^{28}Si fusion reaction [8]. The proton energy calibration is a difficult task with large uncertainties ($\approx$ 10%) as shown by the energy error bars given in Fig. 4. However it does not explain by itself the systematic disagreement between the calculations and the data. This disagreement still remains an open question. The slopes of the proton distribution tails, which is an estimate of the nuclear temperature of the emitting nuclei, seem to be inconsistent with the α spectra. This means that another phenomenon occurs in the decay chain. Probably the present

statistical-model code is not capable to fully account for the sequential proton emission from the decay chain of α-like nuclei.

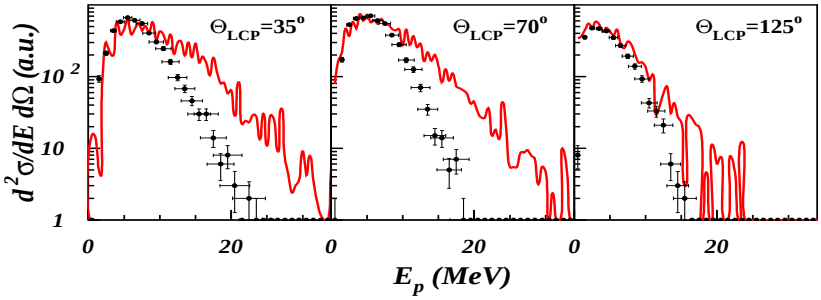

Fig. 4. Experimental (points) and calculated (solid lines) proton spectra for E_{lab} = 96 MeV. The HI's are detected at θ_{lab}=-15° and the coincident protons at the indicated angles.

3.4. α angular correlations

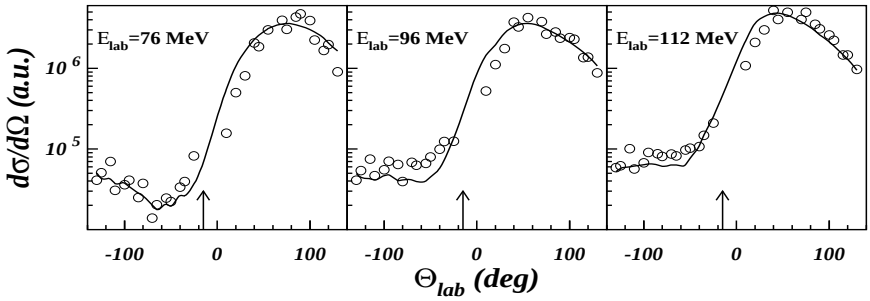

Fig. 5. Experimental (open points) and calculated (solid lines) α angular correlations for the three indicated ^{16}O bombarding energies. The HI's are detected at θ_{lab}=-15° as indicated by the arrows.

The calculated α angular correlations are found to be insensitive to the choice of the Yrast line description. Although the angular correlation data do not constrain the statistical-model parameters, the perfect agreement shown in Fig. 5 for α's (protons correlations are also well predicted) indicates that the present calculations are consistent at least for α-emission.

4. Conclusions

The present analysis indicates that for ^{16}O+^{28}Si the bulk of α yields arises from CN statistical emission. In previous experiments [4,8] the oc-

curence of ^{8}Be cluster emission has been seen in the α spectra and has been interpreted as the result of an α-transfer mechanism from the ^{12}C target to the projectile. A massive ^{8}Be transfer from ^{16}O to ^{28}Si is not observed in the present data. The description of the α particle spectra in the framework of the statistical model indicates strong deformation effects in the ^{44}Ti CN with axis ratios consistent with superdeformation. This dynamic deformation, reached at L_{cr}, has to be distinguished from the static deformation observed in γ-ray spectroscopy. According to the weakly populated SD rotational bands discovered in ^{40}Ca [9], it will be of interest to extend the existing ^{44}Ti level scheme to higher spins with the use of large γ-ray multidetector arrays. Work is in progress to explain the unexpected discrepancies observed for the proton spectra, in particular with the future investigation with ICARE of the ^{32}S+^{12}C reaction which populates the same ^{44}Ti CN.
Acknowlegements: One of us (P. P.) would like to thank the Zakopane Summer School organizing comitee for giving him the opportunity to present his Ph.D. Thesis work. The authors wish to thank the VIVITRON staff, M.A. Saettel for preparing the targets, and J. Devin and C. Fuchs for the excellent support in carrying out this experiment.

Energy [MeV]	E* [MeV]	L_{cr} [$\hbar$]	δ_1	δ_2	b/a-a/c
76	67.1	31	$4.7{\cdot}10^{-4}$	$1.0{\cdot}10^{-7}$	1.9-2.0
96	79.9	34	$4.7{\cdot}10^{-4}$	$1.0{\cdot}10^{-7}$	2.1-2.2
112	90.1	35	$4.7{\cdot}10^{-4}$	$1.0{\cdot}10^{-7}$	2.2-2.3

Table 1. Deformability parameters and axis ratios extracted from Eqs. 1-3.

[1] G. Viesti *et al.*, Phys. Rev. C **38**, 2640 (1988).

[2] J. R. Huizenga *et al.*, Phys. Rev. C **40**, 668 (1989).

[3] C. Bhattacharya *et al.*, Phys. Rev. C **65**, 014611 (2002).

[4] M. Rousseau *et al.*, Phys. Rev. C **66**, 034612 (2002).

[5] C.D. O'Leary *et al.*, Phys. Rev. C **61**, 064314 (2000).

[6] R.A. Zingarelli *et al.*, Phys.Rev. C **48**, 651 (1993).

[7] B. Fornal *et al.*, Phys. Rev. C **44**, 2588 (1991).

[8] M. Rousseau Ph.D. Thesis, Strasbourg University (2000), Rep. IReS **01-02**.

[9] E. Ideguchi *et al.*, *Phys. Rev. Lett.* **87**, 222501 (2001).